

Characterisation of flow conditions for contact erosion analysis using PIV

H.M.D Harshani, S.A Galindo-Torres & A.Scheuermann
School of Civil Engineering, The University of Queensland, Australia

ABSTRACT: The aim of this paper is to examine the flow characteristics at the initiation of contact erosion. When water flows through fine soil to a coarser soil layer, changes of the flow properties may occur due to transition of the pore structure. A pore scale experiment was developed in order to explore the local flow behaviour which leads to migration of fine particles into a coarse structure. Optical access to the pore structure was obtained by having a transparent soil model consisting of hydrogel beads. This allowed water to be used as the fluid phase and resulted in a more adaptable Particle Image Velocimetry (PIV) system. Upward seeded flow was applied to the test section and illuminated using a low risk Light Emitting Diode (LED) light sheet. After calibrating the set-up with macroscopic flow rate measured by flow meter, images of the contact zone of coarse and fine particles were taken with different flow boundary conditions using a high speed camera. Qualitative and quantitative analysis were carried out to identify spatial variability of the flow conditions which led to initiation of the fine particle movement. Results show that the local reorientation of the flow will lead to local initiation of the contact erosion. Major reasons for this behaviour are discussed in this paper.

1 INTRODUCTION

Internal erosion is a severe threat for water retaining structures like embankment dams, dykes and levees. Worldwide, this problem causes a serious threat to the safety of those structures and statistics reveal that it causes failure of approximately half of embankment dams and levees (Foster et al. 2000). When water flows through the granular structure which consists of several soil layers, fine particles are easily detached and transported through the pores of the coarse particles. This leads to small settlements of the structure and finally breach of structure occurs. Through several types of internal erosion, contact erosion is initiated at the interface between two soil layers due to seepage flow. Initiation of the movement of those fine particle depends on the hydraulic, mechanic and geometric conditions at a particle level. Therefore, it is of paramount importance to identify the micro scale parameters causing onset of this phenomena. This will provide a significant contribution for ensuring the stability of water retaining structures.

Contact erosion phenomena with seepage flow parallel to the interface has been studied in laboratories at the sample scale which is considered representative behaviour at the global scale (Cyril et al. 2009). Initiation of erosion has been identified from the non-zero turbidity measurements of outlet water. Visual observations have been limited to the permeameter wall as the porous medium is optically opaque. Beguin et al.

(2012) introduced a transparent soil medium combined with Particle Image Velocimetry (PIV) to characterise the flow at the interface of contact erosion for parallel flow. Statistical analysis was carried out to predict the shear stress distribution an the interface. Contact erosion with a flow perpendicular to the interface has been studied numerically by Galindo-Torres et al. (2013) using Discrete Element Method (DEM) and Lattice Boltzmann Method (LBM).

Though PIV has been considered the dominant measurement technique for flow measurements (Patil and Liburdy 2013, Westerweel et al. 2013), this technique has been rarely used for flow characterization in internal erosion. Beguin et al. (2012) have successfully used this technique to visualize micro scale flow properties at the interface of two soil layer related to contact erosion. To capture the flow field, the porous medium should be transparent and this optical access is obtained by matching the refractive index of the solid and fluid mediums. This technique is called the Refractive Index Matching (RIM) and has been extensively reviewed by Wiederseiner et al. (2011) and Dijkman et al. (2012). In most cases reported in the literature, glass beads were used as the solid phase and fluid has been tuned as mixtures of silicon oil, glycerol or any other mineral oil to achieve the transparency of the medium (Saleh et al. 1993, Huang et al. 2008, Patil and Liburdy 2013, Beguin et al. 2012). These fluid mixtures change their optical properties with time during the experiment which

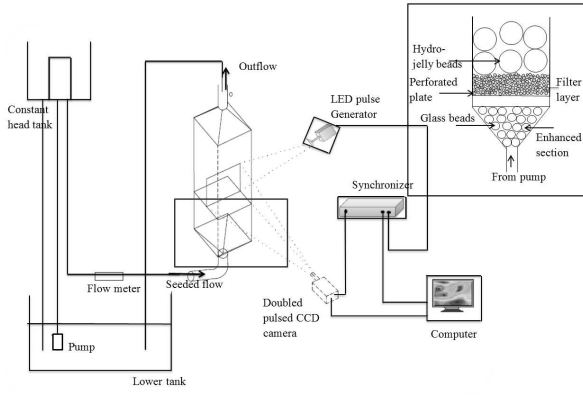


Figure 1: Schematic arrangement of the experimental set-up

is especially due to the sensitivity of their rheological properties with temperature. Another issue of the PIV system for these studies is that flow has been illuminated with the aid of a high power laser which is bulky, expensive and has safety issues. Several studies have been done to investigate the possibility of replacing the laser light sheet with a high power LED light sheet (Ch etelat and Kim 2002, Estevadeordal and Goss 2005, Willert et al. 2010, Buchmann et al. 2012). In those studies, this technique has been widely discussed and successfully used to measure the flow velocity in micro fields less than $10\text{ mm} \times 10\text{ mm}$ Field of View (FOV)s. Estevadeordal and Goss (2005) expanded their study using Particle Shadow Velocimetry (PSV) up to 25 mm FOV.

In this work, an alternative experimental approach is proposed, which is more adaptable and consists of fewer safety issues, to study the pore scale flow characteristics at the onset of contact erosion due to a seepage flow perpendicular to the interface of soil layers. Optical access to the porous medium is obtained by using hydro-gel beads which are made of a super-absorbent polymer, and this allows water to be used as the fluid phase. This allows a more adaptable experimental set-up. Instead of using bulky laser light sheets for the PIV, a LED based light sheet is introduced. This paper discusses the viability of this experimental set-up for studying the of initiation of contact erosion. Experimental set-up and flow field visualization results are described in Section 2 and 3, respectively. Section 4 concludes the study.

2 EXPERIMENTAL SET-UP

Porous medium is placed inside a rectangular column ($10\text{ cm} \times 10\text{ cm} \times 30\text{ cm}$) with conical openings in both sides. Flow across the channel is supplied through a constant head tank filled by water pumped from a lower tank. Porosity of the porous medium is measured using a general volume measurement of 0.4. Flow is measured by a flow meter controlled by a valve. Ployamide Seeding Particles (PSP) of $10\mu\text{m}$ diameter density of 1.03 g/cm^3 are used to seed the flow. Seeding density is maintained at 20 mg/l in order to avoid trapping seeding particles in low velocity

Table 1: Characteristics of the packing

Parameter	Value
Channel size	$10\text{cm} \times 10\text{cm} \times 30\text{cm}$
Coarse particle size	9mm
Fine particle size	1mm
Seeding particle	$15\mu\text{m}$
Fluid density	1000kg/m^3
Sample length	100mm

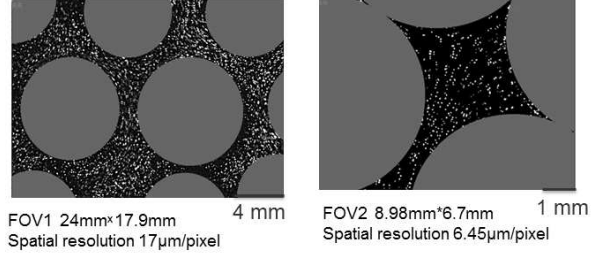


Figure 2: Spatial resolution of two different scales used for the study

regions and the plane of a test section is illuminated using a LED light sheet. Figure 1 is a schematic diagram of the experimental set-up.

Light from the illuminated seeding particle inside the porous medium is captured by a CCD camera. The camera sensor consists of 1392×1040 pixels with a $6.45 \times 6.45\ \mu\text{m}$ pixel size and 14 bit dynamic range. It has the capability of a minimum $1\ \mu\text{s}$ inter frame time and readout time of the first image can be adjusted between $5\ \mu\text{s}$ to 60 s . Spatial resolution of the images plays a major role for micro scale flow characteristics. Two different FOVs are selected as shown in Figure 2 with $17\ \mu\text{m}/\text{pixel}$ and $6.45\ \mu\text{m}/\text{pixel}$ spatial resolutions for FOV1 and FOV2, respectively. This helps to scan different pore structures with different spatial resolution in order to track local flow characteristics. Double exposure images are processed using cross correlation of the velocity field. Image pairs are captured with known time interval (δt) between light sheets and this parameter is carefully tuned according to the velocity of the flow. A synchroniser is used to control the camera shutter speed and δt . Each image is divided into sub-regions referred to as Interrogation Windows (IW)s as achieve in Figure 3. Eight-ten particles should be within an IW to achieve good results (Raffel et al. 2013). During statistical PIV, it is assumed that all particles in an IW move a similar distance and direction. The velocity vector per each IW

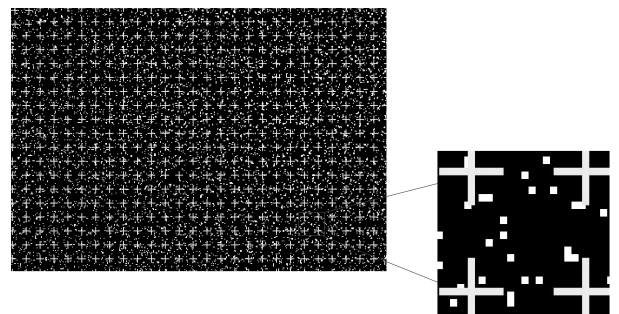


Figure 3: View of the interrogation window with group of seeding particles

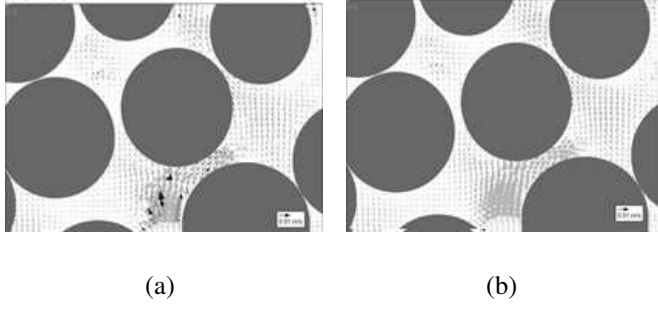


Figure 4: Velocity vector fields for different correlation methods (a) single pass interrogation (b) multi-pass interrogation combining with grid refining technique

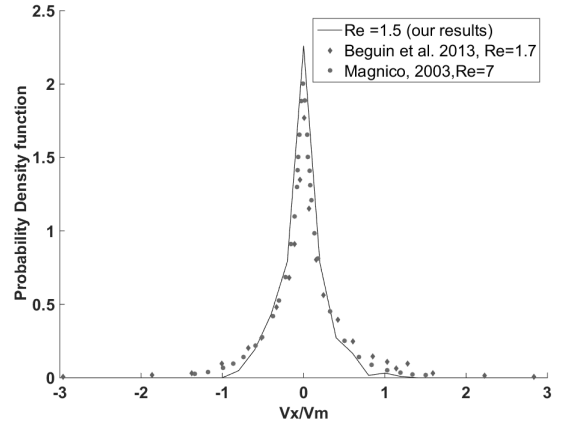
is then computed with the aid of mathematical correlation using average displacement while PIVView 2C software is used for image analysis.

During the pre-processing step a high pass filter is applied to remove low frequency background variations and it is combined with thresholding. A thresholding value of 150 is used to produce a final image with the same intensity for the all particles. This will result in all particles having the same contribution to the correlation function. Simple ruler measurements are used to convert pixel measurements to real space measurements. The Magnification factor is calculated using this calibration constant. In order to calculate the seed image diameter (d_τ) in the image plane, geometric and diffractions effects are considered. Effective seed image diameter (d_τ) is given by, $d_\tau = \sqrt{M^2 d_p^2 + d_s^2}$, where, M is the image magnification, d_p is the seeding particle diameter in the object palne and d_s is the defraction limited spot size given by, $d_s = 2.44(1+M)\frac{f}{D}\lambda$. The ratio $\frac{f}{d}$ is the f-number of the camera lens and λ is the wavelength of the illumination light. Corresponding d_τ is 2.57 pixels which helps to prevent the peak locking adding effect (Raffel et al. 2013).

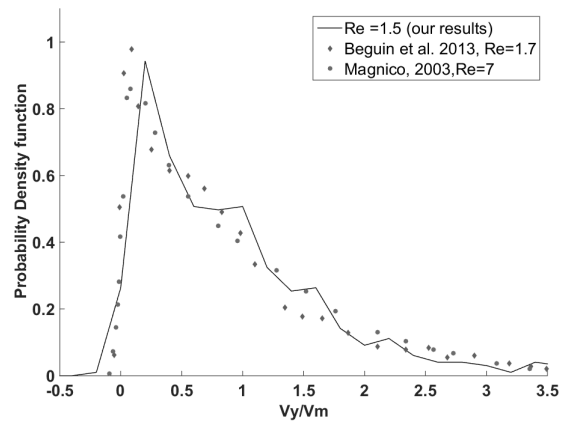
3 RESULTS AND DISCUSSION

3.1 PIV Optimisation

During the correlation analysis for finding the velocity vector, a displacement peak should be obtained according to the particle displacement within the IW. In a steady flow, a constant displacement can be seen for all IWs and the size of the IW can be selected in a way that all particles in the IW of image 1 exist in the IW of image 2. As porous flow is more heterogeneous, different velocity gradients per image can be found. To capture those characteristics into one frame, the correlation process should be optimised rather than using a single pass correlation (Raffel et al. 2013). Thus a multi-pass interrogation system combined with a grid refining system is introduced to reduce the loss of pairs of particles within the IW. Figure 4 shows the accuracy of those methods for a velocity vector field for different velocity gradients.



(a)



(b)

Figure 5: Histograms for (a) normalised vertical velocity (b) normalised horizontal velocity

Following those improvements, velocity vector fields are analysed quantitatively for the flow field through mono-dispersed packing.

3.2 Quantitative analysis

In order to compare the results with the available literature data, statistical distributions of the velocity field are obtained. Histograms for vertical velocity V_y and horizontal velocity V_x are plotted for $Re=1.5$. The Reynolds number (Re) defined as $Re = \rho V_m d / \mu$ where d is diameter of particles and ρ and μ are the density and viscosity of water, respectively. $V_m (=Q/A)$ is the mean Darcy velocity through the medium. Volumetric flow rate Q is measured by flow meter and the cross sectional area of bed A is $10 \text{ cm} \times 10 \text{ cm}$. For comparison with the literature records, histograms are plotted against a non-dimensionalised parameter which is obtained by dividing V_y and V_x by the mean velocity V_m (Figure 5). The normalized longitudinal velocity distribution (V_y/V_m) shows a decay in positive velocity. Normalized transverse velocity distribution (V_x/V_m) shows a peak close to zero and symmetry

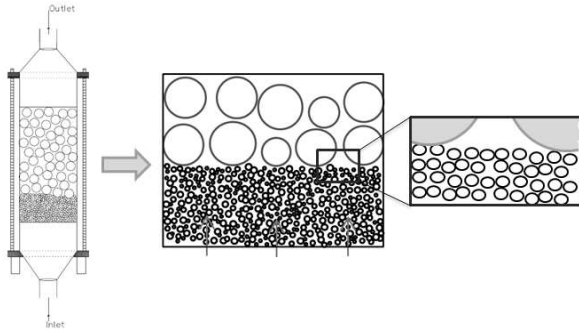


Figure 6: Pore scale view of the transition region interesting for the initiation of contact erosion

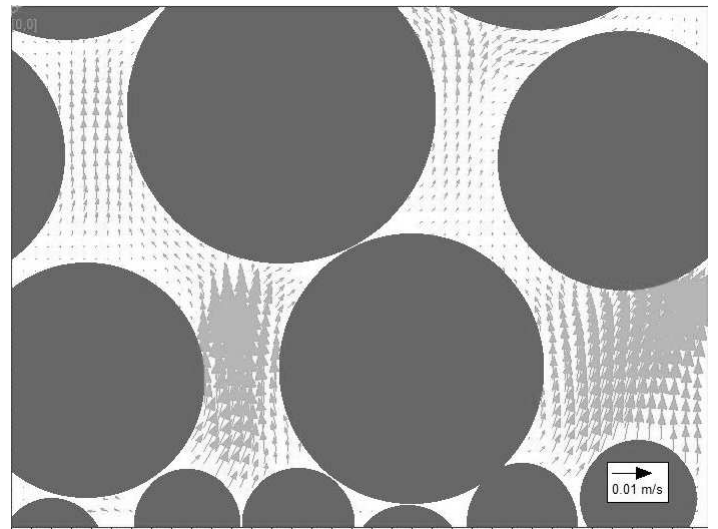
along the axis as expected since it is not a preferential direction. Similar trends have been reported by Be-guin et al. (2012) and Magnico (2003).

3.3 Contact Erosion Studies

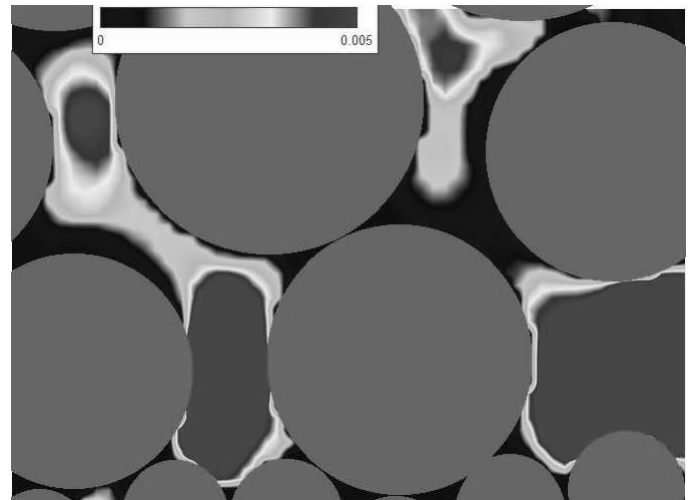
The next task is to apply these flow visualization procedures to a study of contact erosion. When water flows from a fine layer to a coarse layer, flow properties may change significantly due to changes of porosity. It is interesting to understand the flow characteristics happening at the interface at this transition zone. As shown in Figure 6, the flow conditions that lift fine particles up should be identified to understand the onset of contact erosion. To model this phenomena hydrogel beads are placed over a packing of small glass beads of 1 mm diameter which models the fine layer.

Figure 7 shows the image taken at the the interface of fine and coarse materials. As the glass beads do not have the same refractive index as water, the transparent nature of the porous medium can not be obtained and thus, any flow characteristics can not be captured inside the fine layer. Flow characteristics just above the fine layer (transition region) can be analyzed and compared with the flow in the coarse layer. Figure 7(a) shows the velocity vector map of the flow. It is interesting to see that a high flow exists fine layer and gradually decreases its velocity into coarse layer. These jet-like flow conditions may affect the stability of the fine particles. Figure 7(b) shows a contour plot for the velocity distribution and clearly indicates the high intensity flows present at the transition zone.

To further analyse the flow behaviour in this region FOV2 is used to scan various pore geometries with high spatial resolution. Figure 8 highlights a very interesting flow characteristic that directly affects to the stabilization of fine particles. The flow existing the fine layer changes flow direction according to the constriction inlets directed into that pore. Due to the presence of the large void space, horizontal directional flow dominates and the vectors show vortex like flow around the fine particles. This may lead to a rotation of fine particles before that lift up during the onset of erosion. This characteristics has been already identified by Harshani et al. (2015) in numerical simulations. Also Galindo-Torres et al. (2013) has modelled contact erosion for upward flow using DEM and



(a)



(b)

Figure 7: Flow condition changes when it transit from fine layer to coarse layer (a)Velocity vector map (b)Contour plot related to velocity magnitude

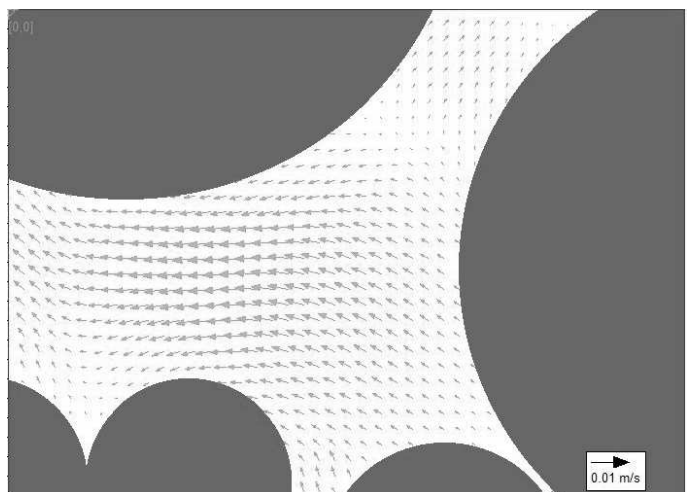


Figure 8: Flow velocity vectors just above the fine layer captured by FOV2

LBM. They concluded that angular momentum transferred to the fine particles by the fluid affects their mobility into larger voids.

One major difficulty encountered during this experimental study is the difficulty of capturing three dimensional flow. Some pore velocities inside pores obstructed by particles shows zero or misleading velocity vectors due to disappearance of the seeding particles from measuring the plane. This is due to the transverse flow perpendicular to the plane. Another problem is that the seeding particles tend to be glued to the surface of the beads after conducting several experimental runs. Therefore, the porous pack should be washed after several tests. Thus, the same pore structures cannot be maintained during the whole period of the experiment which affects replication of the experiment. As porosity has had the same value these packing changes do not affect the final statistical results. Hydrogel beads should be kept in clear water when not in use, to maintain their same size and shape.

4 CONCLUSIONS

A novel approach to PIV experiments for porous flow has been introduced using hydrogel beads and LED based light sheet. Despite a few limitations of using hydrogel beads discussed earlier, these two changes lead to a more adaptable PIV experiment set-up with high safety procedures use for pore scale contact erosion studies. Results show that this high power LED light sheet is very promising for flow illumination. Vertical and horizontal velocity measurements are in good agreement with the literature. Velocity intensities are found to be high in the transition zone between fine and coarse layer. Flow characteristics which disturb the stability of the fine layer are identified. This experimental set-up will be used for further contact erosion studies with introduction of transparent material to the fine layer. This will allow the characterisation of the flow not only in the transition zone but also in the fine layer.

5 ACKNOWLEDGEMENTS

The presented research is part of the Discovery Project (DP120102188) Hydraulic erosion of granular structures: Experiments and computational simulations funded by the Australian Research Council.

REFERENCES

Beguin, R., P. Philippe, & Y.-H. Faure (2012). Pore-scale flow measurements at the interface between a sandy layer and a model porous medium: Application to statistical modeling of contact erosion. *Journal of Hydraulic Engineering* 139, 1–11.

Buchmann, N. A., C. E. Willert, & J. Soria (2012). Pulsed, high-power led illumination for tomographic particle image velocimetry. *Experiments in fluids* 53, 1545–1560.

Chételat, O. & K. C. Kim (2002). Miniature particle image velocimetry system with led in-line illumination. *Measurement Science and Technology* 13(7), 1006.

Cyril, G., F. Yves-Henri, B. Rémi, & H. Chia-Chun (2009). Contact erosion at the interface between granular coarse soil and various base soils under tangential flow condition. *Journal of Geotechnical and Geoenvironmental Engineering* 136, 741–750.

Dijksman, J. A., F. Rietz, K. A. Lőrincz, M. van Hecke, & W. Losert (2012). Invited article: Refractive index matched scanning of dense granular materials. *Review of Scientific Instruments* 83, 011301.

Estevadeordal, J. & L. Goss (2005). Piv with led: particle shadow velocimetry (psv). In *43rd AIAA aerospace sciences meeting and exhibit, meeting papers*.

Foster, R. M., F. Robin, & S. Matt (2000). The statistics of embankment dam failures and accidents. *Canadian Geotechnical Journal* 37, 1000–1024.

Galindo-Torres, S. A., A. Scheuermann, H. B. Mühlhaus, & D. J. Williams (2013). A micro-mechanical approach for the study of contact erosion. *Acta Geotechnica*, 1–12.

Harshani, H. M. D., S. A. Galindo-Torres, A. Scheuermann, & H. B. Mühlhaus (2015). Micro-mechanical analysis on the onset of erosion in granular materials. *Philosophical Magazine* 95, 3146–3166.

Huang, A. Y., M. Y. F. Huang, H. Capart, & R.-H. Chen (2008). Optical measurements of pore geometry and fluid velocity in a bed of irregularly packed spheres. *Experiments in Fluids* 45, 309–321.

Magnico, P. (2003). Hydrodynamic and transport properties of packed beds in small tube-to-sphere diameter ratio: pore scale simulation using an eulerian and a lagrangian approach. *Chemical Engineering Science* 58, 5005–5024.

Patil, V. A. & J. A. Liburdy (2013). Flow characterization using piv measurements in a low aspect ratio randomly packed porous bed. *Experiments in Fluids* 54, 1–19.

Raffel, M., C. E. Willert, J. Kompenhans, et al. (2013). *Particle image velocimetry: a practical guide*. Springer.

Saleh, S., J. F. Thovert, & P. M. Adler (1993). Flow along porous media by partial image velocimetry. *AIChE Journal* 39, 1765–1776.

Westerweel, J., G. E. Elsinga, & R. J. Adrian (2013). Particle image velocimetry for complex and turbulent flows. *Annual Review of Fluid Mechanics* 45, 409–436.

Wiederseiner, S., N. Andreini, G. Epely-Chauvin, & C. Ancey (2011). Refractive-index and density matching in concentrated particle suspensions: a review. *Experiments in fluids* 50, 1183–1206.

Willert, C., B. Stasicki, J. Klinner, & S. Moessner (2010). Pulsed operation of high-power light emitting diodes for imaging flow velocimetry. *Measurement Science and Technology* 21, 075402.